ACS APPLIED MATERIALS & INTERFACES

Research Article

www.acsami.org

Nanoscale Electrical and Mechanical Characteristics of Conductive Polyaniline Network in Polymer Composite Films

Shadi Jafarzadeh,*[,†] Per M. Claesson,[†,‡] Per-Erik Sundell,[§] Jinshan Pan,[†] and Esben Thormann[∥]

[†]Division of Surface and Corrosion Science, Department of Chemistry, School of Chemical Science and Engineering, KTH Royal Institute of Technology, Drottning Kristinas väg 51, 100 44 Stockholm, Sweden

[‡]Chemistry, Materials and Surfaces, SP Technical Research Institute of Sweden, P.O. Box 5607, 114 86 Stockholm, Sweden

[§]SSAB EMEA, 781 84 Borlänge, Sweden

[∥]Department of Chemistry, Technical University of Denmark, Kemitorvet 207, 2800 Kongens Lyngby, Denmark

ABSTRACT: The presence and characteristics of a connected network of polyaniline (PANI) within a composite coating based on polyester acrylate (PEA) has been investigated. The bulk electrical conductivity of the composite was measured by impedance spectroscopy. It was found that the composite films containing PANI have an electrical conductivity level in the range of semiconductors (order of 10^{-3} S cm^{-1}), which suggests the presence of a connected network of the conductive phase. The nanoscopic distribution of such a network within the cured film was characterized by PeakForce tunneling atomic force microscopy (AFM). This method simultaneously provides local information about surface topography and nanomechanical properties, together with electrical conductivity arising from conductive paths connecting the metallic substrate to the surface of the coating. The data demonstrates that a PEA-rich layer exists at the composite−air interface, which hinders the conductive phase to be fully detected at the surface layer. However, by exposing the internal structure of the composites using a microtome, a much higher population of a conductive network of PANI, with higher elastic modulus than the PEA matrix, was observed and characterized. Local current−voltage (I−V) spectroscopy was utilized to investigate the conduction mechanism within the nanocomposite films, and revealed non-Ohmic characteristics of the conductive network.

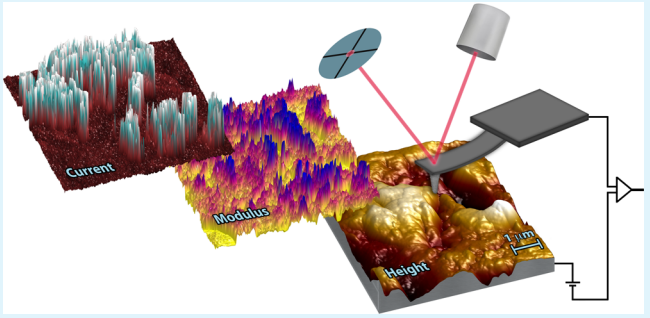

KEYWORDS: *conducting polymer, polyaniline, conductive network, PeakForce TUNA AFM*

1. INTRODUCTION

Composites of conducting polymers, specifically polyaniline (PANI), in a polymeric matrix are receiving considerable interest in many applications,[1,2] among which anticorrosive coatings[3−5] are of particular interest in this work. The active corrosion protection offered by these composites has been suggested to be due to the reversible reduction−oxidation (redox) property of PANI with its equilibrium potentials being more positive than most commonly used metals.[6] As a result, PANI can ennoble the metal surface and facilitate formation of a thin protective passive oxide layer at the metal-coating interface.[5,7,8] Moreover, in case of defects in the coating, PANI may help in providing a second physical barrier of a passivating complex made by reaction between (metal) cations and (doping) anions released by PANI.[9] All these actions are effective only if the conductive phase is in galvanic contact with the metal substrate through connected paths spanning along and across the coating depth.[3,4] The presence of such a continuous network in various systems has been macroscopically tested by bulk conductivity measurements using different techniques.[10−12] The distribution of conductive domains within PANI films[13,14] or composite films containing conducting polymers[15−17] has been investigated by local mapping of the current flow using conductive atomic force microscopy (AFM), where surface spots with electrical contact to the metal substrate show a high signal in the current map. By this technique, one can detect the conducting polymer that is located at the outermost surface and at the same time is connected to a pathway allowing high current flow to the metal substrate. However, this technique is unable to distinguish the conducting polymer from the coating matrix if the conducting path is isolated and not in electrical contact with the substrate. A further limitation with conventional conductive AFM measurements is that it is operated in contact mode, where sample or tip damage and tip contamination may occur due to significant lateral and normal forces. This also makes it difficult to image soft samples. PeakForce quantitative nanomechanical (QNM) AFM is a relatively new powerful technique to

Received: August 2, 2014
Accepted: October 8, 2014
Published: October 8, 2014

quantitatively measure the nanomechanical variations in nanocomposites.[18−23] Here properties like surface elastic modulus can be derived from tip−sample force curves, providing an elasticity image at the same time as a topography image is obtained. Images of other properties, such as tip−surface adhesion and surface deformation are also obtained simultaneously, and all problems with lateral forces are eliminated. With this technique, one can distinguish between different components in a composite coating like, in our case, PANI and PEA but without knowing if the detected PANI at the surface is electrically connected to the substrate under the film.

In this work, we utilized PeakForce Tunneling AFM (TUNA), a technique that combines the benefits of conductive AFM and PeakForce QNM to simultaneously measure the surface nanomechanical and local electrical properties of conductive polymeric nanocomposites based on UV-curable PEA matrix and conducting PANI. The formation of a continuous conductive network through the film may be affected by many factors in the composite design and preparation. We have previously studied the effects of the PANI particle size and shape,[24] dispersion properties,[24] PANI−PANI and PANI−matrix interactions[25] and UV curing conditions.[26] Here, the nanoscopic distribution of the conductive phase and characteristics of the charge conduction through the current pathways is reported.

2. EXPERIMENTAL SECTION

2.1. Materials. The composite coatings studied in this work were based on polyaniline (PANI) conducting polymer dispersed in a polyester acrylate (PEA) matrix. PANI was synthesized by the so-called "rapid mixing" method, discussed in detail in another work.[24] The reaction relies on chemical oxidative polymerization of aniline (Aldrich grade, 99%) with ammonium peroxodisulfate (Merck grade, 99%) as an oxidant, in the presence of phosphoric acid (Sigma-Aldrich, 99%) aqueous solution as a dopant. This polymer will be referred to as "PANI-PA", where PA stands for the phosphoric acid dopant. The polymer matrix (PEA) was based on a chlorinated polyester acrylate resin mixed with 40 wt % 1,6-hexanediol diacrylate monomer (laboratory formulation Ebecryl 584 from Cytec Surface Specialties). This UV-curable formulation also contains 5 wt % free radical photoinitiators (a blend of 3 parts 1-Hydroxycyclohexyl phenyl ketone, Additol CPK from Cytec Surface Specialties, with 2 parts 2,4,6-Trimethylbenzoyldiphenylphosphine oxide, Lucirin TPO-L from BASF) and 5 wt % of a methacrylate modified acidic adhesion promoter (Ebecryl 171, Cytec Surface Specialties).

2.2. Preparation and Application of Composite Coatings. The proper method to design and prepare the composite coatings used in this study has been established after detailed studies on properties of the composite components individually and within the blend before and after UV curing.[24−26] PANI-PA, softened in acetone in an ultrasonic bath, was added to the PEA formulation in small portions under pearl-milling with a speed of 3000 rpm. By this procedure, despite the viscous media, homogeneous PEA/PANI dispersions of 3 and 10 wt % PANI-PA content with good UV curing capability could be made.[26] The blends were applied on polished carbon steel using a spin-coater (Headway Research Inc.) and cured under high intensity UV lamps, a combination of Hg and Ga Fusion lamps giving a total intensity of around 1.5 W cm^{-2}, and a UV dose of 1.2 J cm^{-2}, in the UV-A region. The dry thickness of the cured films was measured to be about 10 μm by a digital thickness meter (MiniTest 3100 from ElektroPhysik, Germany).

On some of the cured films, a thin layer (a few micrometers) was removed from the outer surface in order to allow investigation of the internal composite structures. The removal of the top layer was done using a microtome, LEICA SM2500 from LEICA Microsystems, Nussloch, GmbH, equipped with a diamond blade.

2.3. Characterization Techniques. *2.3.1. Impedance Spectroscopy.* Bulk electrical conductivity measurements were performed by impedance spectroscopy using a Solartron 1296 electrochemical interface coupled to a Solartron 1260 frequency response analyzer. The impedance was measured at room temperature with 1 s integration with an AC amplitude of 100 mV while the frequency was swept from 1 MHz to 1 Hz with 5 points/decade. The samples were placed tightly between two gold plate electrodes connected to the instrument. The measurements were repeated after different time intervals until a stable condition was reached, and the data was collected and analyzed by the SMaRT software, from Solartron Analytical. The measured impedance modulus, R, was then converted to bulk electrical conductivity, σ, data using $\sigma = ((4l)/(\pi d^2 \cdot R))$, where l is the thickness and d the diameter of the sample. The electrical conductivity was measured on pressed pellets of PANI-PA (with 0.15 cm thickness and 1.28 cm diameter) and also on 10 μm thick composite films of PEA with 0, 3 and 10 wt % PANI-PA content applied on polished carbon steel.

2.3.2. PeakForce TUNA Atomic Force Microscopy (AFM). Nanometer scale lateral resolution images of surface topography, surface nanomechanical properties and electrical conductivity were obtained simultaneously using atomic force microscopy (AFM) (Multimode, Nanoscope V from Bruker, USA) operating in PeakForce tunneling mode. Conductive Pt-coated rectangular silicon cantilevers (DPE15/NO Al, Mikromasch) with nominal spring constant of 46 N/m and a tip radius of <40 nm (determined more precisely for each used cantilever) were employed in this study. PeakForce tapping is an imaging mode that simultaneously provides quantitative mapping of surface material properties together with topography.[18−23] This mode allows imaging with a controlled feedback force and eliminates lateral forces, which reduces the risk of sample damage and tip contamination. Briefly, the surface position is modulated by a sine wave with an amplitude of approximately 150 nm and a frequency of 1 kHz. During each period of oscillation, the surface is moved into contact with the AFM tip and the feedback electronics adjust the averaged surface position such that the maximum cantilever deflection (the peak force) equals a predetermined setpoint value. The applied force setpoint has been chosen during each experiment so that the sample surface is deformed a few nanometers, which is optimal in order to calculate the elastic modulus of the surface layer without losing too much lateral resolution.[23] By calibration of the optical lever sensitivity and the cantilever spring constant, information about cantilever deflection and piezo position can be converted to force vs distance curves describing the tip−sample interaction during approach and separation.[27] From such a force curve, one can for example determine the elastic modulus of the sample by fitting the Derjaguin−Muller−Toporov (DMT) model[28,29] to the part of the force curve where the sample and tip are in contact:

$$F = \frac{4}{3}E^*\sqrt{Rd^3} + F_{adh}$$

Here, F is the force, R is the tip radius, d is the deformation value at a given force, F_{adh} is the maximum adhesion force, and $E^* = [((1 - \nu_s^2)/E_s) + ((1 - \nu_{tip}^2)/E_{tip})]^2$ is the effective elastic modulus. In the equation for E^*, E_s and E_{tip} are Young's modulus of the sample and tip, respectively, and ν is the Poisson's ratio. In this study, we have determined the tip radius by an indirect method where the radius was adjusted to fit the DMT model for a sample with known elastic modulus (polystyrene, E = 2.7 GPa). In PeakForce tapping, a new set of approach and retraction force versus separation curves are obtained during each period of oscillation (every 1 ms). This means that, as the sample is scanned, an image showing the variation in elastic modulus is obtained simultaneously with the image providing topographical information. In PeakForce tunneling AFM (TUNA), a current amplifier (TUNA module) is added to the system to measure the current signal while a voltage is applied to the sample substrate. It should be noted that it is not sufficient that the tip is in contact with a conductive material but an electrical connection to the (conductive) metal substrate under the film is essential for the current to flow. Thus, a current signal is obtained only if the tip during the sample contact

constitutes a part of a closed electrical circuit which, in our case, means that a network of PANI should span from the metal substrate to the conductive AFM-tip. It is noteworthy that the TUNA module is collecting the current signal within the short time of one PeakForce tapping cycle (a fraction of 1 ms). Figure 1 illustrates a plot of force

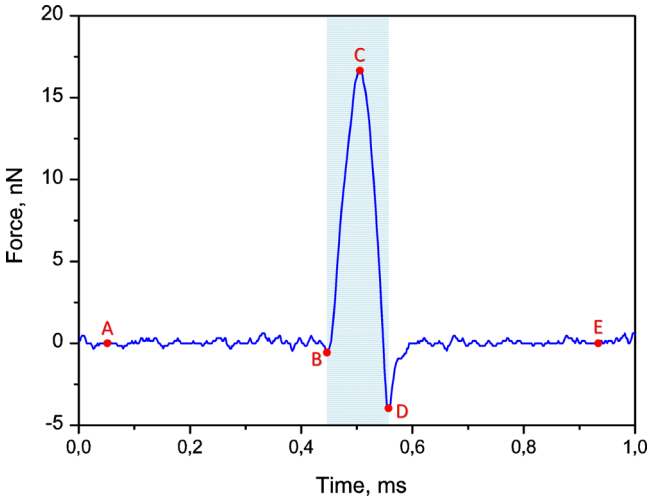

Figure 1. Force versus time plot obtained during one PeakForce tapping cycle on PEA/PANI-PA composite coatings. At points A and E, the tip is far from the surface and the current flow is zero. At point B, the tip jumps into contact to the surface and, at point D, it pulls off the surface. Point C represents the maximum reached force, i.e., the PeakForce setpoint. The contact current is being collected during the highlighted time period, i.e., from point B to D.

versus time obtained during one cycle on our composite coatings. The highlighted area represents the time period during which the tip is in contact with the sample and the contact current is being collected.

With PeakForce TUNA, we simultaneously collected information on topography, elastic modulus and local electrical current. Depending on the level of measured current, the current sensitivity of the TUNA module was switched between 20 and 100 pA/V, and a bias voltage ranging between 7 and 9 V was applied. Besides PeakForce TUNA imaging, the AFM was also used in spectroscopy mode to investigate the current–voltage (I–V) characteristics at selected surface positions in order to quantify the variations of the local conductance. Here, the tip was pressed against the sample with a constant force, i.e., feedback switched to contact mode, and the voltage was linearly ramped up and down while the current signal was collected. Analysis of the AFM images and I–V curves was performed with the Nanoscope Analysis V1.40 software (Bruker, USA).

3. RESULTS AND DISCUSSION

3.1. Bulk Electrical Conductivity. The electrical conductivity versus frequency at room temperature for PANI-PA pellet and PEA/PANI-PA composite films applied on polished carbon steel are shown in Figure 2. At frequencies below approximately 10 kHz, a constant value independent of frequency is reached. The electrical conductivity at these low frequencies is equivalent to the DC-conductivity, which is related to the interconnectedness of the conductive species.

It is found that the electrical conductivity of PANI-PA at a frequency of 1 Hz is on the order of 10^{-2} to 10^{-1} S cm^{-1} (range of good semiconductors), which is consistent with the values reported in the literature.[24,30] The bulk electrical conductivity of PEA (plot not shown here) is on the order of 10^{-12} S cm^{-1} (range of insulators). By adding a few percent PANI-PA to PEA, composites with electrical conductivity on the order of 10^{-3} S cm^{-1} are achieved. This relatively high conductivity of

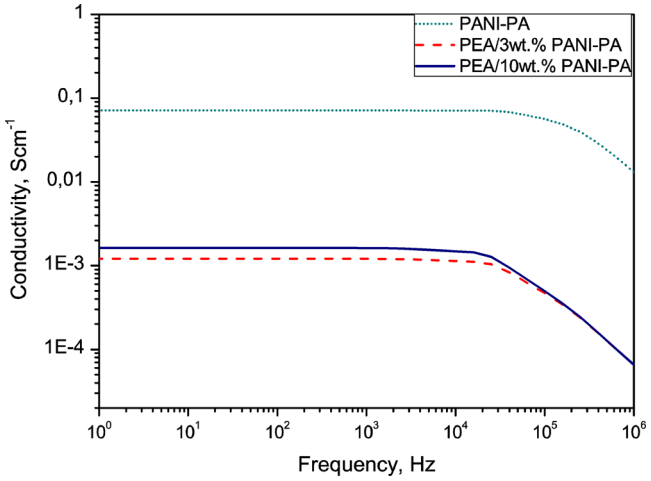

Figure 2. Electrical conductivity versus frequency for PANI-PA and PEA/PANI-PA composite films with 3 and 10 wt % PANI-PA content. The conductivity is calculated from the data obtained by impedance spectroscopy at room temperature.

the composites suggests the presence of a continuous network of a PANI phase across the coating depth. The electrical conductivity level of the composite is only slightly increased by increasing the PANI-PA content from 3 to 10 wt %, which suggests that both studied concentrations are above the percolation threshold and it is the intrinsic properties and conduction mechanism within the formed conductive network that is dominantly deciding the conductivity range of the composites. For composites with 3 and 10 wt % PANI, the center-to-center distance of particles in 100 nm spherical form[24] would be approximately 580 and 390 nm, respectively, if the particles were sitting in a perfect cubic lattice. In this case, a connected network would not be present. However, no particular attractive or repulsive interaction has been detected between PANI-PA particles in liquid PEA resin in earlier works[24,25] and, thus, the particles are expected to be distributed randomly. In a random distribution, a percolated network of particles may be achieved in agreement with the high electrical conductivity measured above. A schematic illustration of the suggested network structure is shown in Figure 3.

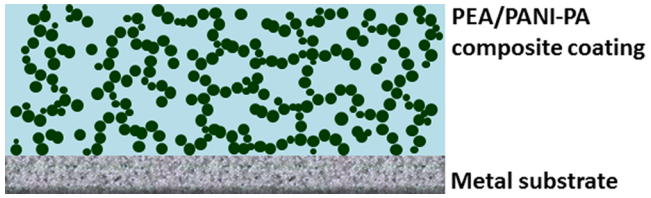

Figure 3. Schematic illustration of a network structure of PANI-PA spherical nanoparticles in PEA matrix.

3.2. Local Probing of Surface Nanomechanical Properties and Electrical Conductivity. *3.2.1. Pure Components.* In the first step, the nanomechanical properties of the pure components (PEA and PANI-PA) were characterized. To this end, uniform films of PEA coated on polished carbon steel and pressed pellets of PANI-PA were used as substrates for PeakForce tapping mode AFM imaging. Figure 4 displays the AFM topography, elastic modulus and deformation images of these two materials taken in air with a scan size of 2 × 2 μm.

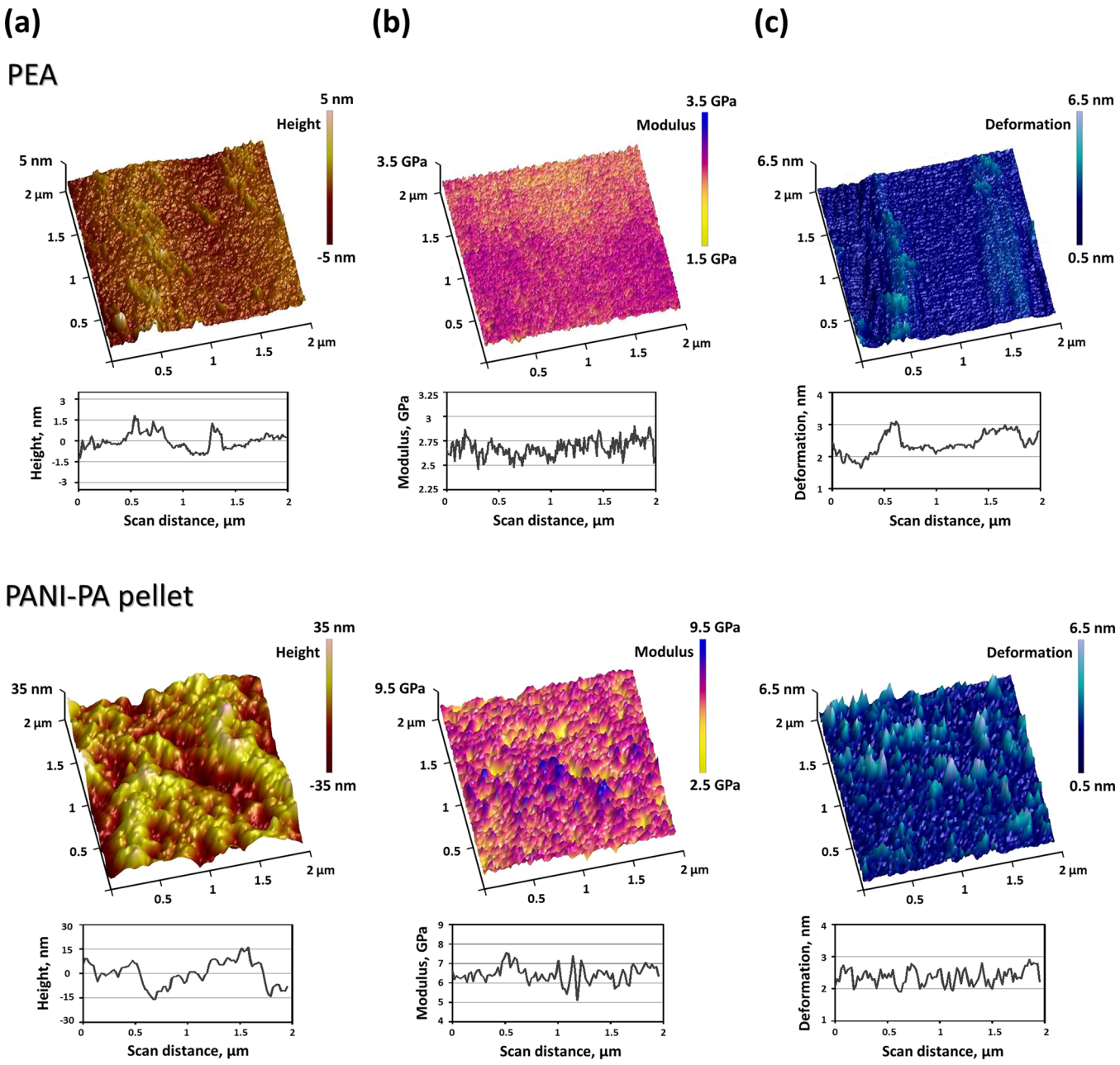

Figure 4. (a) Topography, (b) DMT modulus and (c) deformation images and line scan profiles (from the middle of each image) for a uniform film of PEA (first row) and a pressed pellet of PANI-PA (second row). The images were recorded in air using PeakForce AFM.

The values of the modulus demonstrate that PEA is significantly softer than PANI-PA. The mean value of the modulus for PEA was found to be 2.6 GPa, whereas a value of 6.3 GPa was found for PANI-PA. This difference allows us to distinguish these two materials when studying the composites in the following experiments. As discussed in the Experimental Section, the PeakForce setpoint was in each case adjusted to achieve a surface deformation of a few nanometers (see Figure 4c).

3.2.2. Composite–Air Interface. Composite films with 10 wt % PANI-PA content were chosen for AFM studies, on which many areas of the surface were scanned in order to obtain representative data. In most areas, the current level was too low to be detected. Some regions of very low conductivity (current signal up to a few pA) were found, and the modulus on these regions was close to the level for PEA rather than for PANI-PA. This suggests the presence of a thin layer of PEA on top of the conductive phase that lowers both the modulus and the measured conductivity. The preferential depletion of PANI-PA particles from the coating-air interface is due to the favorable interaction between PEA and PANI-PA.[24]

Moreover, a low population of conductive spots isolated by large insulating regions was observed at the surface layer. These spots represent aggregates of PANI-PA sticking out from the surface (exemplified in Figure 5), as judged from the high conductivity and high modulus detected. A scan line across one of these areas is shown as an inset in Figure 5, which reveals a modulus value similar to that measured on pressed PANI-PA pellets, surrounded by regions showing the modulus level of PEA.

3.2.3. Composite Internal Structure. The results of the PeakForce TUNA AFM imaging on the PEA/PANI-PA

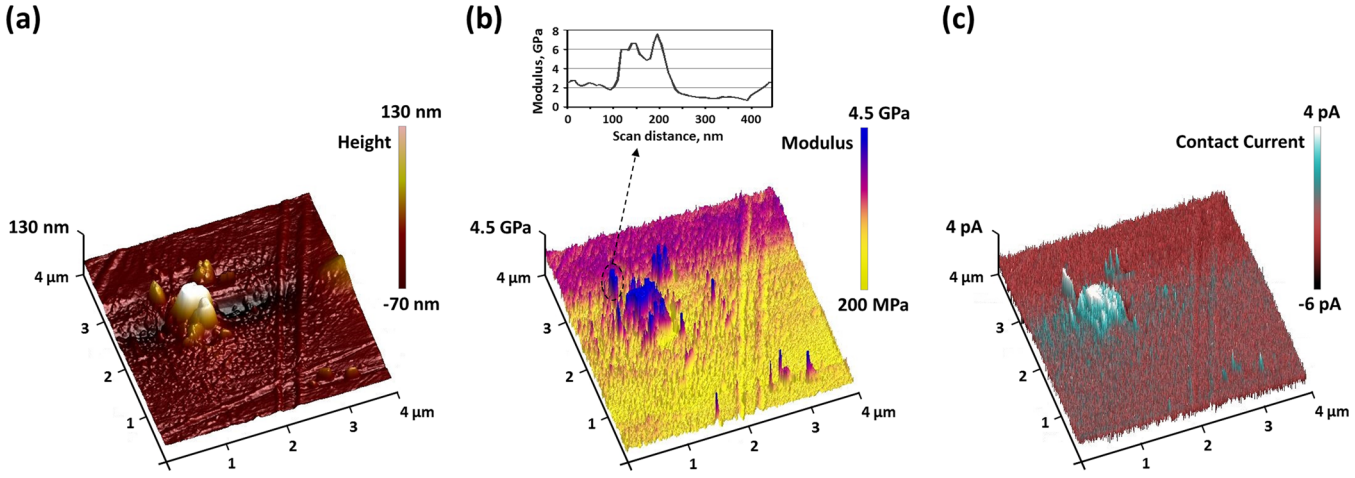

Figure 5. PANI-PA aggregates sticking out of the PEA matrix at the coating-air interface. (a) Topography, (b) DMT modulus and (c) current maps, with a line scan profile over a part of the modulus image (inset). The PEA/PANI-PA composite film was applied on polished carbon steel. The images were recorded in air using PeakForce TUNA AFM.

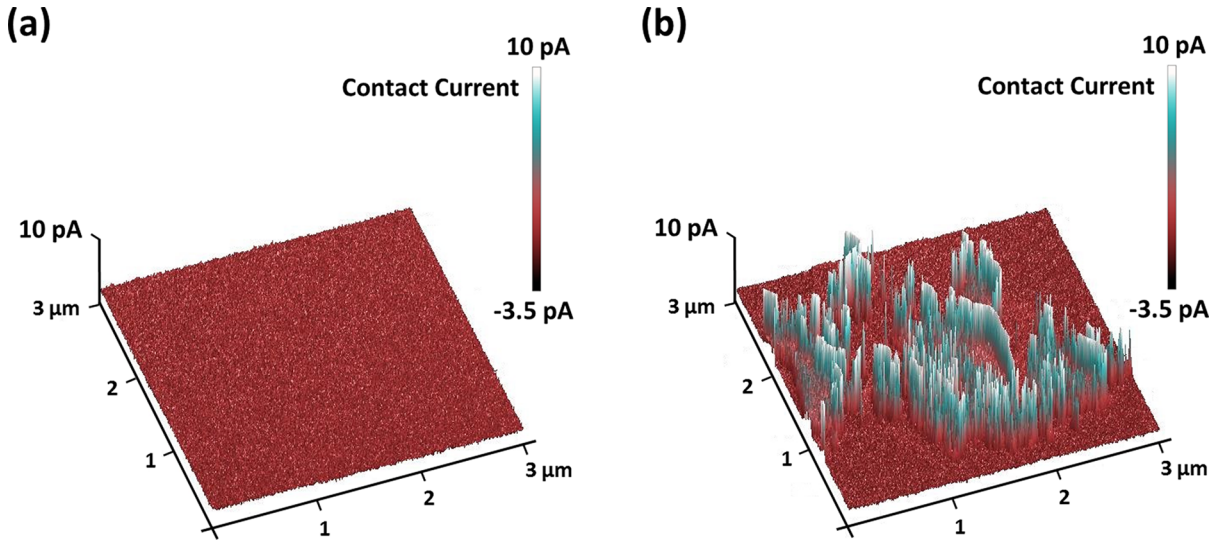

Figure 6. Current maps of microtomed films of (a) PEA and (b) PEA/PANI-PA applied on polished carbon steel. The images were recorded in air using PeakForce TUNA AFM.

composite film surfaces suggest that PEA is preferentially present at the coating−air interface, but that a conductive network nevertheless spans from the few PANI-PA particles located at this surface down to the metal substrate below the coating. To visualize this network, one needs to remove the top layer of the coating, which was achieved by using a microtome. The exposed internal surface area was then investigated using PeakForce TUNA AFM.

Current maps of 3 × 3 μm internal surface areas of microtomed PEA and PEA/PANI-PA films are shown in Figure 6. As expected, no conductive spots/network is observed for the insulating PEA film (Figure 6a). In contrast, a high fraction of the internal surface of the PEA/PANI-PA composite displays significant electrical conductivity (Figure 6b). The conductive phase illustrates the connected network of PANI-PA particles formed within the coating, and the relative high current signal obtained suggests electrical connection of this network to the metal substrate.

Similar connected network structures of PANI-PA within the insulating PEA matrix are observed on all scanned surfaces after microtoming. The high area fraction with high current flow on a larger scan area of 6 × 6 μm is illustrated in Figure 7(a−c). Here, the distribution of the conductive phase with high current is evidently associated with regions with high modulus (consistent with the level measured for PANI-PA). It should also be noted that some areas with high modulus show zero conductivity in the corresponding current map. This can be explained by considering that some parts of the exposed PANI-PA network are not in electrical contact to the metal substrate, which thus prevents the current from flowing across the film. PeakForce TUNA imaging can therefore not only distinguish between the different components in the composite film, via the elastic modulus but also determine the fraction of the PANI-PA phase that is part of a connected network. The current map of the composites internal structure (presented in Figure 7c) can be compared to a 10 × 10 μm image of the original coating−air interface, where local conductivity is only observed over a small fraction of the surface area and with much lower magnitude due to the presence of a thin layer of PEA on top (Figure 7d).

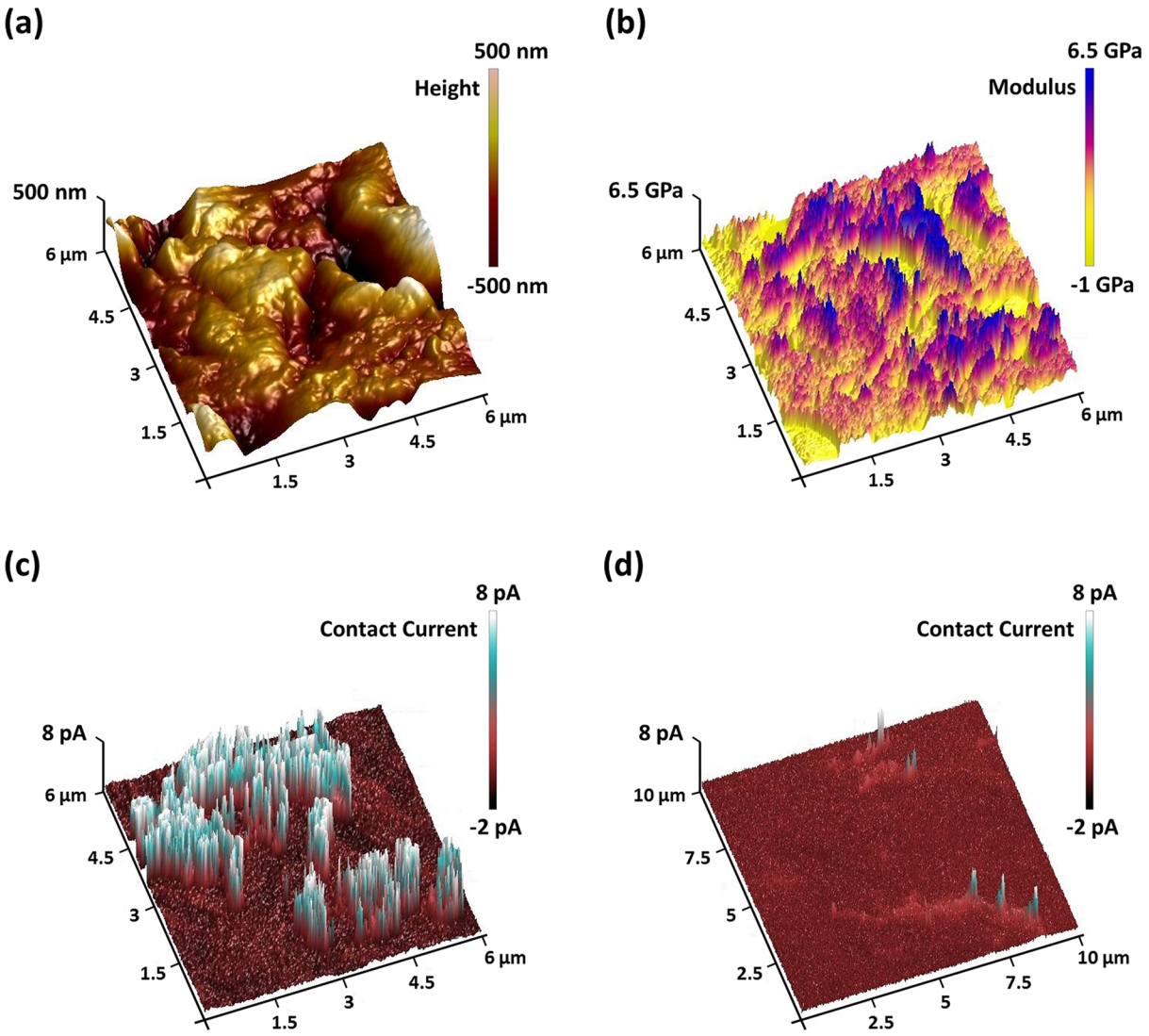

Figure 7. (a) Topography, (b) DMT modulus, and (c) current maps on a microtomed area and (d) current map on an area before microtoming on PEA/PANI-PA composite films applied on polished carbon steel. The images were recorded in air using PeakForce TUNA AFM.

3.3. Current–Voltage Characteristics of the Conductive Domains. Representative $I-V$ curves recorded on different spots of a PANI-PA pellet surface and, for comparison, on a polished carbon steel surface are shown in Figure 8a. PANI-PA displays an Ohmic response, with a resistance ($R = V/I$) significantly higher than carbon steel. Furthermore, the $I-V$ curves are rather symmetrical with respect to 0 V. Although PANI is considered as a semiconductor, Ohmic characteristics have previously been seen for fully doped conducting polymers,[17,31] and this result thus indicates good conductivity and conducting homogeneity of our synthesized polymer.

Figure 8b shows a number of $I-V$ curves obtained on selected conductive spots of the PEA/PANI-PA composite film. The shape of these $I-V$ curves reveals a non-Ohmic behavior, apparently similar to that of semiconductors,[32] where no or a very low current flow is detected when the magnitude of the applied bias voltage is lower than a certain threshold. A reason for the non-Ohmic behavior and the related threshold value, which in semiconductor theory is known as the energy band gap, could be the presence of a thin PEA layer surrounding individual PANI particles that makes the electron transfer across particle–particle contacts non-Ohmic.[33] The high probability of PANI-PA particles being covered by a thin layer of PEA has previously been suggested,[24] based on the observation that liquid PEA shows good wettability on PANI-PA as a result of attractive interfacial interaction (negative interfacial energies) between these two materials. It has furthermore been suggested that PANI-PA particles can get close enough to provide interparticle electrical conduction. This suggestion originates from data obtained by direct measurements of interactions,[25] where only very short-range repulsive forces and absence of any attraction between PANI-PA particles within the liquid PEA matrix was demonstrated. Closely packed particles of several tens of nanometers have also been visualized within the bulk of PEA/PANI-PA composites (SEM images in ref 25). Together with these previous obtained results, the $I-V$ characteristics observed in this work therefore suggests that the conduction mechanism is hopping of the charge carriers between conductive particles with (mostly) no direct physical contact.[12] The hopping conduction mechanism for the charge transport between distant sites within blends of PANI and insulating polymers have been suggested in the literature[34,35] and been interpreted in terms of Mott's model for three-dimensional conductance.[36] The $I-V$ curves presented in

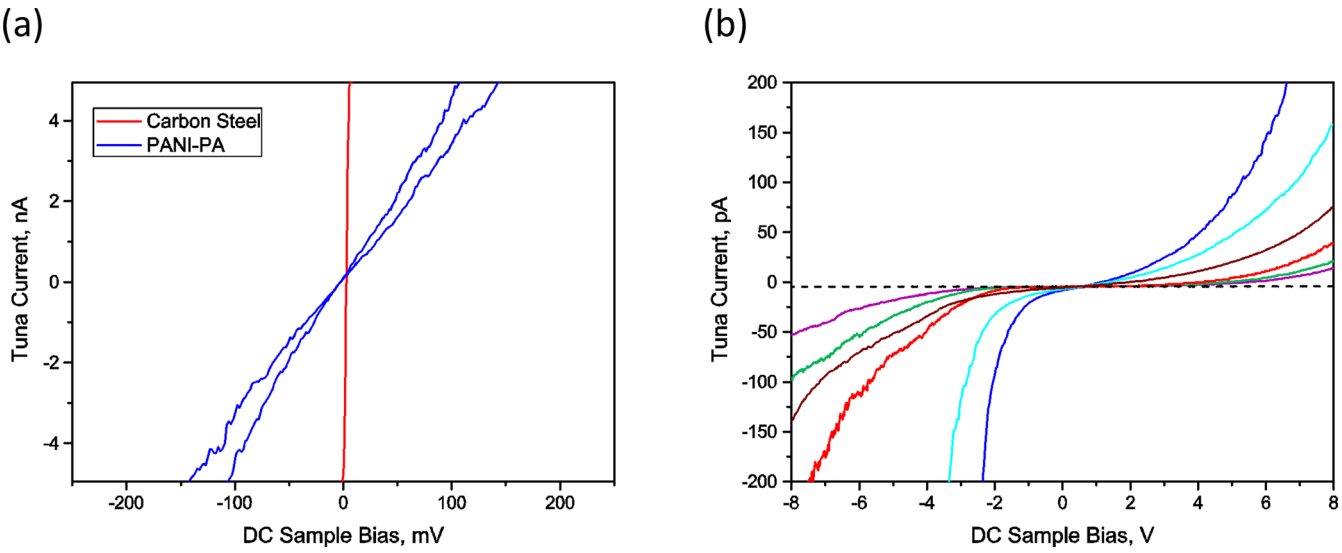

Figure 8. *I*−*V* curves for (a) PANI-PA and carbon steel, and (b) various spots on a microtomed PEA/PANI-PA composite film. The dashed black line in panel b represents an *I*−*V* curve recorded on an insulating area on a PEA/PANI-PA composite film before microtoming. The current passing through this area is essentially zero over the whole range of applied bias voltage (−8 to +8 V). The *I*−*V* curves are obtained by AFM-based *I*−*V* spectroscopy, where the current is measured under a constant force and an applied bias voltage that is linearly ramped down.

Figure 8b reveal that the magnitude of energy band gap varies for different surface positions on the microtomed PEA/PANI-PA composite film surface, ranging from 2 eV down to sub eV. This is consistent with the above-suggested conduction mechanism because the inhomogeneity in the distribution of the conducting phase within the composite will naturally lead to variations in the local PANI-PA interparticle separations and thus in the values of the energy band gaps. Finally, it is also seen that most of the *I*−*V* curves measured on our conductive composites are not symmetrical with respect to 0 V. Similar asymmetric features of *I*−*V* curves showing higher current at one polarity than the other have previously been reported[17] and suggested to be related to the asymmetry of the conductivity in the junction between a metal and a pure semiconductor.[37] However, because PANI-PA shows symmetrical *I*−*V* curves while characterized as a pure material, we postulate that the asymmetry is also related to the suggested conduction mechanism, and not to the semiconductive nature of PANI-PA itself. Another consideration could be the reversible redox property of PANI, as it may be partially reduced or oxidized under a large negative or positive voltage, respectively. This behavior could also have contributed to the asymmetry of the *I*−*V* curves obtained under a wide range of applied voltage on PEA/PANI-PA composites.

4. CONCLUSIONS

The presence of conductive networks within composite films containing polyaniline has been suggested by the measured level of bulk conductivity being in the range of semiconductors (order of 10^{-3} S cm^{-1}). Distribution and characteristics of such networks were directly observed by PeakForce TUNA AFM imaging. A low population of conductive regions is detected on the surface layer of the composite films while conductive PANI-rich areas with high elastic modulus are observed on the coating internal structure exposed by using a microtome. The results confirm the presence of a continuous network of the conductive phase in the composite coatings and depletion of PANI-PA at the composite−air interface due to the favorable interaction between PEA and PANI-PA. The presence of such a conductive network is essential to have the whole PANI content involved in the expected active corrosion protection. *I*−*V* curves reveal an Ohmic behavior for pure PANI-PA but non-Ohmic characteristics for the composite films, suggesting that the PANI-PA particles are not in Ohmic contact but surrounded by a PEA layer that is thin enough to allow electrical conduction between neighboring PANI-PA particles.

AUTHOR INFORMATION

Corresponding Author

*S. Jafarzadeh. Address: Division of Surface and Corrosion Science, Department of Chemistry, School of Chemical Science and Engineering, KTH Royal Institute of Technology, Drottning Kristinas väg 51, 100 44 Stockholm, Sweden. Tel: +46-87906670. Fax: +46-8208284. E-mail: shadijz@kth.se.

Notes

The authors declare no competing financial interest.

ACKNOWLEDGMENTS

This research was supported by the SSF program: Microstructure, Corrosion and Friction Control, and by Jernkontoret, Sweden. E.T. also acknowledges the Swedish Research Council (VR) for financial support. Ann-Sofie Olovsson from Akzo Nobel Industrial Finishes AB is acknowledged for providing the UV curing facilities. Kenneth Möller from SP Technical Research Institute of Sweden is thanked for helping with the microtoming.

REFERENCES

(1) Bhadra, S.; Khastgir, D.; Singha, N. K.; Lee, J. H. Progress in Preparation, Processing and Applications of Polyaniline. *Prog. Polym. Sci.* **2009**, *34*, 783−810.

(2) Pud, A.; Ogurtsov, N.; Korzhenko, A.; Shapoval, G. Some Aspects of Preparation Methods and Properties of Polyaniline Blends and Composites with Organic Polymers. *Prog. Polym. Sci.* **2003**, *28*, 1701−1753.

(3) Jafarzadeh, S.; Adhikari, A.; Sundall, P.-E.; Pan, J. Study of PANI-MeSA Conducting Polymer Dispersed in UV-Curing Polyester

Acrylate on Galvanized Steel as Corrosion Protection Coating. *Prog. Org. Coat.* **2011**, *70*, 108−115.
(4) de Souza, S. Smart Coating Based on Polyaniline Acrylic Blend for Corrosion Protection of Different Metals. *Surf. Coat. Technol.* **2007**, *201*, 7574−7581.
(5) Sathiyanarayanan, S.; Muthkrishnan, S.; Venkatachari, G. Corrosion Protection of Steel by Polyaniline Blended Coating. *Electrochim. Acta* **2006**, *51*, 6313−6319.
(6) Tallman, D.; Spinks, G.; Dominis, A.; Wallace, G. Electroactive Conducting Polymers for Corrosion Control. *J. Solid State Electrochem.* **2002**, *6*, 73−84.
(7) Nguyen, T. D.; Nguyen, T. A.; Pham, M. C.; Piro, B.; Normand, B.; Takenouti, H. Mechanism for Protection of Iron Corrosion by an Intrinsically Electronic Conducting Polymer. *J. Electroanal. Chem.* **2004**, *572*, 225−234.
(8) Schauer, T.; Joos, A.; Dulog, L.; Eisenbach, C. D. Protection of Iron Against Corrosion with Polyaniline Primers. *Prog. Org. Coat.* **1998**, *33*, 20−27.
(9) Pereira da Silva, J. E.; Córdoba de Torresi, S. I.; Torresi, R. M. Polyaniline Acrylic Coatings for Corrosion Inhibition: The Role Played by Counter-Ions. *Corros. Sci.* **2005**, *47*, 811−822.
(10) Paul, R. K.; Pillai, C. K. S. Melt/Solution Processable Polyaniline with Functionalized Phosphate Ester Dopants and Its Thermoplastic Blends. *J. Appl. Polym. Sci.* **2001**, *80*, 1354−1367.
(11) Ameen, S.; Ali, V.; Zulfequar, M.; Mazharul Haq, M.; Husain, M. Electrical and Spectroscopic Characterization of Polyaniline−Polyvinyl Chloride (PANI−PVC) Blends Doped with Sodium Thiosulphate. *Phys. B (Amsterdam, Neth.)* **2008**, *403*, 2861−2866.
(12) Ebrahim, S. Electrical Transport Mechanism in Polyaniline/Formvar Blend Films. *High Perform. Polym.* **2009**, *21*, 468−483.
(13) Barrière, F.; Fabre, B.; Hao, E.; LeJeune, Z. M.; Hwang, E.; Garno, J. C.; Nesterov, E. E.; Vicente, M. G. H. Electropolymerizable 2,2′-Carboranyldithiophenes. Structure−Property Investigations of the Corresponding Conducting Polymer Films by Electrochemistry, UV−Visible Spectroscopy and Conducting Probe Atomic Force Microscopy. *Macromolecules* **2009**, *42*, 2981−2987.
(14) Sutar, D. S.; Tewari, R.; Dey, G. K.; Gupta, S. K.; Yakhmi, J. V. Morphology and Structure of Highly Crystalline Polyaniline Films. *Synth. Met.* **2009**, *159*, 1067−1071.
(15) Planès, J.; Houzé, F.; Chrétien, P.; Schneegans, O. Conducting Probe Atomic Force Microscopy Applied to Organic Conducting Blends. *Appl. Phys. Lett.* **2001**, *79*, 2993−2995.
(16) Alexeev, A.; Loos, J.; Koetse, M. M. Nanoscale Electrical Characterization of Semiconducting Polymer Blends by Conductive Atomic Force Microscopy (C-AFM). *Ultramicroscopy* **2006**, *106*, 191−199.
(17) Lee, H. J.; Lee, J.; Park, S.-M. Electrochemistry of Conductive Polymers. 45. Nanoscale Conductivity of PEDOT and PEDOT:PSS Composite Films Studied by Current-Sensing AFM. *J. Phys. Chem. B* **2010**, *114*, 2660−2666.
(18) Sababi, M.; Kettle, J.; Rautkoski, H.; Claesson, P. M.; Thormann, E. Structural and Nanomechanical Properties of Paperboard Coatings Studied by Peak Force Tapping Atomic Force Microscopy. *ACS Appl. Mater. Interfaces* **2012**, *4*, 5534−5541.
(19) Bodvik, R.; Thormann, E.; Karlson, L.; Claesson, P. M. Temperature Responsive Surface Layers of Modified Celluloses. *Phys. Chem. Chem. Phys.* **2011**, *13*, 4260−4268.
(20) Rico, F.; Su, C.; Scheuring, S. Mechanical Mapping of Single Membrane Proteins at Submolecular Resolution. *Nano Lett.* **2011**, *11*, 3983−3986.
(21) Foster, B. New Atomic Force Microscopy (AFM) Approaches Life Sciences Gently, Quantitatively, and Correlatively. *Am. Lab.* **2012**, *44*, 24−28.
(22) Sweers, K.; van der Werf, K.; Bennink, M.; Subramaniam, V. Nanomechanical Properties of Alpha-Synuclein Amyloid Fibrils: A Comparative Study by Nanoindentation, Harmonic Force Microscopy, and Peakforce QNM. *Nanoscale Res. Lett.* **2011**, *6*, 270.
(23) Pittenger, B.; Erina, N.; Su, C. Quantitative Mechanical Property Mapping at the Nanoscale with PeakForce QNM; Bruker Application Note #128; Bruker Nano Surfaces Division: Santa Barbara, CA, 2012. http://www.bruker.com/fileadmin/user_upload/8-PDF-Docs/SurfaceAnalysis/AFM/ApplicationNotes/AN128-RevB0-Quantitative_Mechanical_Property_Mapping_at_the_Nanoscale_with_PeakForceQNM-AppNote.pdf.
(24) Jafarzadeh, S.; Thormann, E.; Rönnevall, T.; Adhikari, A.; Sundell, P.-E.; Pan, J.; Claesson, P. M. Toward Homogeneous Nanostructured Polyaniline/Resin Blends. *ACS Appl. Mater. Interfaces* **2011**, *3*, 1681−1691.
(25) Jafarzadeh, S.; Claesson, P. M.; Pan, J.; Thormann, E. Direct Measurement of Colloidal Interactions between Polyaniline Surfaces in a UV-Curable Coating Formulation: The Effect of Surface Hydrophilicity/Hydrophobicity and Resin Composition. *Langmuir* **2014**, *30*, 1045−1054.
(26) Jafarzadeh, S.; Johansson, M.; Sundell, P.-E.; Claudino, M.; Pan, J.; Claesson, P. M. UV-Curable Acrylate-based Nanocomposites: Effect of Polyaniline Additives on the Curing Performance. *Polym. Adv. Technol.* **2013**, *24*, 668−678.
(27) Thormann, E.; Pettersson, T.; Claesson, P. M. How to Measure Forces with Atomic Force Microscopy without Significant Influence from Nonlinear Optical Lever Sensitivity. *Rev. Sci. Instrum.* **2009**, *80*, 093701.
(28) Butt, H.-J.; Cappella, B.; Kappl, M. Force Measurements with the Atomic Force Microscope: Technique, Interpretation and Applications. *Surf. Sci. Rep.* **2005**, *59*, 1−152.
(29) Cappella, B.; Dietler, G. Force-Distance Curves by Atomic Force Microscopy. *Surf. Sci. Rep.* **1999**, *34*, 1−104.
(30) Blinova, N. V.; Stejskal, J.; Trchová, M.; Prokeš, J. Control of Polyaniline Conductivity and Contact Angles by Partial Protonation. *Polym. Int.* **2008**, *57*, 66−69.
(31) Cho, S. H.; Kim, D.; Park, S.-M. Electrochemistry of Conductive Polymers: 41. Effects of Self-Assembled Monolayers of Aminothiophenols on Polyaniline Films. *Electrochim. Acta* **2008**, *53*, 3820−3827.
(32) Wu, C.-G.; Chang, S.-S. Nanoscale Measurements of Conducting Domains and Current−Voltage Characteristics of Chemically Deposited Polyaniline Films. *J. Phys. Chem. B* **2004**, *109*, 825−832.
(33) Trionfi, A.; Scrymgeour, D. A.; Hsu, J. W. P.; Arlen, M. J.; Tomlin, D.; Jacobs, J. D.; Wang, D. H.; Tan, L.-S.; Vaia, R. A. Direct Imaging of Current Paths in Multiwalled Carbon Nanofiber Polymer Nanocomposites using Conducting-Tip Atomic Force Microscopy. *J. Appl. Phys.* **2008**, *104*, 083708.
(34) Ebrahim, S. M.; Kashyout, A. B.; Soliman, M. M. Electrical and Structural Properties of Polyaniline/Cellulose Triacetate Blend Films. *J. Polym. Res.* **2007**, *14*, 423−429.
(35) M, R.; Yoon, C. O.; Yang, C. Y.; Moses, D.; Smith, P.; Heeger, A. J.; Cao, Y. Transport in Polyaniline Networks Near the Percolation Threshold. *Phys. Rev. B* **1994**, *50*, 13931−13941.
(36) Mott, N. F.; Davis, E. A. *Electronic Processes in Non-Crystalline Materials*; Oxford University Press: Oxford, U. K., 1979.
(37) Chang, S.-S.; Wu, C.-G. Effects of Polymerization Media on the Nanoscale Conductivity and Current−Voltage Characteristics of Chemically Synthesized Polyaniline Films. *J. Phys. Chem. B* **2005**, *109*, 18275−18282.